NUMERICAL SIMULATION OF 3-D FRACTIONAL-ORDER CONVECTION-DIFFUSION PDE BY A LOCAL MESHLESS METHOD

by

Hari Mohan SRIVASTAVA [a,b,c,*], ***Hijaz AHMAD*** [d], ***Imtiaz AHMAD*** [e], ***Phatiphat THOUNTHONG*** [f], ***and Muhammad Nawaz KHAN*** [e]

[a] Department of Mathematics and Statistics, University of Victoria, Victoria, B. C., Canada
[b] Department of Medical Research, China Medical University Hospital, China Medical University, Taichung, Taiwan, China
[c] Department of Mathematics and Informatics, Azerbaijan University, Baku, Azerbaijan
[d] Department of Basic Sciences, University of Engineering and Technology, Peshawar, Khyber Pakhtunkhwa, Pakistan
[e] Department of Mathematics, University of Swabi, Khyber Pakhtunkhwa, Pakistan
[f] Renewable Energy Research Centre, Department of Teacher Training in Electrical Engineering, Faculty of Technical Education, King Mongkut's University of Technology North Bangkok, Bangsue, Bangkok, Thailand

Original scientific paper
https://doi.org/10.2298/TSCI200225210S

In this article, we present an efficient local meshless method for the numerical treatment of 3-D convection-diffusion PDE. The demand of meshless techniques increment because of its meshless nature and simplicity of usage in higher dimensions. This technique approximates the solution on set of uniform and scattered nodes. The space derivatives of the models are discretized by the proposed meshless procedure though the time fractional part is discretized by Liouville-Caputo fractional derivative. Some test problems on regular and irregular computational domains are presented to verify the validity, efficiency, and accuracy of the method.

Key words: *Liouville-Caputo derivative, meshless method, radial basis function, convection-diffusion equation, irregular domain*

Introduction

Fractional calculus has attracted significant interests in the field of engineering and applied sciences in the last few years. The elementary knowledge of fractional calculus can be found in [1, 2]. Fractional differential equations contain derivatives of any complex or real order, being considered as general form of differential equations. The comprehensive applications in real world problems are described by fractional PDE and it is found to be an effective tool in interpretation and modeling of numerous problems appear in physics and applied mathematics [3-8].

Recently, a great effort has been expended to develop the exact and approximate behavior of fractional PDE. In this effort several enthusiastic methods have been applied for the solution of fractional PDE such as homotopy analysis method [9, 10], expansion methods [11,

* Corresponding author, e-mail: harimsri@uvic.ca

12], homotopy analysis transform method [13], fractional difference method [14], operational method [15], variational iteration method [5, 16-18], homotophy perturbation method [19], direct approach [20, 21], Lie symmetry analysis [22], differential transform method [23], reproducing kernel method [24], extended differential transform [25], local fractional Riccati differential equation method [26], meshless methods [27, 28] and Chebychev spectral method [29].

Different types of meshless techniques have been got expansive consideration for tackling diverse kind of PDE model arises in almost all disciplines of engineering. Especially the radial basis functions (RBF) based meshless methods are one of the most popular type among these methods. The meshless methods, consider a set of scattered and uniform data points on the domain in contrast to some classical mesh-based techniques such as finite difference and finite element methods. Therefore these processes do not require to mesh the domain. Moreover, the uses of RBF [30] increase advantages and preferences of technique due to this property that the RBF only depend on the Euclidian distance between two points of the spatial domain. According to these facts, meshless methods are known as very flexible and useful mathematical tools which can be applied to high dimensional models with irregular and complicated domains. Meshless collocation technique based on the RBF is one of the very popular strong-form meshless methods which is widely employed to many practical problems [31, 32]. Although the classical meshless collocation method based on the globally supported RBF is known as a very efficient computational technique to deal with complicated and high dimensional PDE, but the method leads to an ill-conditioned and dense system of algebraic equations. In the global meshless method, the RBF are used to obtain the coefficients, so that the derivatives of a function $f(x)$ can be written as a linear combination of the functional values at the predetermined nodes. This numerical scheme is simple and effective. However, the approximation can become unstable as the number of collocation points become large resulting in dense matrices. This leads to ill-conditioning and sensitivity to the shape parameters in the RBF formulation. Unfortunately, this ill-conditioning and computational cost of implementation of the technique will increase dramatically by increasing number of the scattered data points. To ward off these deficiencies, the researchers suggested local meshless method (LMM) [33, 34].

The LMM use only neighboring collocation points and it does not have the typical ill-conditioning that comes with large dense matrix systems. Additionally, in such RBF based meshless techniques, the proper selection of RBF as well as shape parameter value play a crucial rule in the convergence. Among these RBF, the multiquadric (MQ) is perhaps the most popular that is used in applications. This is due to its high convergence rate and accuracy. Perhaps a disadvantage that the MQ RBF has as compared to the polyharmonic splines is that the accuracy depends on the correct choice of the shape parameter. The same disadvantage applies to the inverse multiquadric (IMQ) and the Gaussian (GA) RBF as well. Finding the appropriate shape parameter is an ongoing research problem. In local methods, the shape parameter does not vary much, which is beneficial in choosing a good value. Another advantage of the local technique is that the accuracy is not compromised by the computational efficiency. Unlike the global approach where it is required to work with a dense matrix, the local technique results in a sparse matrix which can be solved accurately and efficiently.

In the recent literature, LMM are used for better numerical approximation of complex PDE models [35, 36]. Meshless techniques using RBF are viable alternate numerical mechanisms used for solutions of different types of complicated linear, non-linear, integer and fractional order PDE arising in science and engineering. Different variants of meshless procedures are reported in the literature. Some of the reported work include Mohebbi *et al.* [37] time fractional non-linear Schrodinger equation, Piret and Hanert [38] fractional diffusion equations,

Mohebbi *et al.* [39] 2-D modified anomalous fractional sub-diffusion equation, Hosseini *et al.* [40] fractional telegraph equation, Wei *et al.* [41] 2-D time fractional diffusion equations, Ghehsareh *et al.* [42] 2-D fractional evolution equation, Aslefallah and Shivanian [43] non-linear time-fractional integro-differential reaction-diffusion equation, Kumar *et al.* [44] time fractional diffusion wave equation, Wei *et al.* [45] variable-order time fractional diffusion equation, Dehghan *et al.* [46] time fractional non-linear Sine-Gordon and Klein-Gordon equations and Avazzadeh *et al.* [47] time fractional diffusion-wave equation.

Current research work is devoted to use the LMM for the numerical investigation of 3-D time-fractional convection-diffusion and Burgers' equations. The space derivatives are approximated by the local meshless procedure using the inverse quadric (IQ), MQ, and the GA radial basis functions whereas time fractional part is approximated by using Liouville-Caputo definition. Both rectangular and non rectangular geometries are considered in numerical experiments.

Consider the unsteady time fractional linear convection-diffusion PDE:

$$\frac{\partial^{\alpha} W(\bar{z},t)}{\partial t^{\alpha}} = \beta \nabla W(\bar{z},t) + \gamma \Delta W(\bar{z},t) + F(\bar{z},t) \equiv \mathcal{L} W(\bar{z},t), \quad \bar{z} \in \Omega, \quad 0 < \alpha \le 1, t > 0 \tag{1}$$

with the following initial-boundary conditions:

$$W(\bar{z},0) = W_0 \tag{2}$$

$$\mathcal{C}_1(\bar{z},t) = g_1(\bar{z},t), \quad \bar{z} \in \partial\Omega \tag{3}$$

where β is the diffusion coefficient, and γ the real constants.

Similarly, the time fractional Burgers' equation:

$$\frac{\partial^{\alpha} W(\bar{z},t)}{\partial t^{\alpha}} = \beta \nabla W(\bar{z},t) - \frac{1}{2}\frac{\partial W^2(\bar{z},t)}{\partial x} - \frac{\partial\left\lfloor \frac{3}{2} W(\bar{z},t) - \frac{1}{2} W^2(\bar{z},t) \right\rfloor}{\partial y} -$$

$$- \frac{\partial\left\lfloor \frac{3}{2} W(\bar{z},t) - \frac{1}{2} W^2(\bar{z},t) \right\rfloor}{\partial z}, \quad \bar{z} \in \Omega, \quad 0 < \alpha \le 1, t > 0 \tag{4}$$

with the following initial-boundary conditions:

$$W(\bar{z},0) = W_0 \tag{5}$$

$$\mathcal{C}_2(\bar{z},t) = g_2(\bar{z},t), \quad \bar{z} \in \partial\Omega \tag{6}$$

where β is a diffusion coefficient.

Scheme of the LMM

The LMM [33] is extended to the time fractional convection-diffusion models. The derivatives of $W(\bar{z},t)$ are approximated at the centers $\bar{z}_h$ by the neighborhood of $\bar{z}_h$, $\{\bar{z}_{h1}, \bar{z}_{h2}, \bar{z}_{h3}, \ldots, \bar{z}_{hn_h}\} \subset \{\bar{z}_1, \bar{z}_2, \ldots, \bar{z}_{N^n}\}$, $n_h \ll N^n$, where h = 1, 2,…, N^n. In case of 1-D, $\bar{z} = x$, and for 2-D, $\bar{z} = (x, y)$ and for 3-D case, $\bar{z} = (x, y, z)$. Now, in 1-D case, we have:

$$W^{(m)}(x_h) \approx \sum_{k=1}^{n_h} [\lambda_k^{(m)} W(x_{hk})], \quad h = 1, 2, \ldots, N \tag{7}$$

By substituting RBF $\psi(\| x - x_p \|)$ in eq. (7), we have:

$$\psi^{(m)}(\| x_h - x_p \|) = \sum_{k=1}^{n_h} \lambda_{hk}^{(m)} \psi(\| x_{hk} - x_p \|), \quad p = h_1, h_2, \ldots, hn_h \tag{8}$$

where

$$\psi(\| x_{hk} - x_p \|) = \exp(-\| x_{hk} - x_p \|^2 / c^2), \quad \psi(\| x_{hk} - x_p \|) = [1 + (c \| x_{hk} - x_p \|)^2]^{-1}, \text{ and}$$

$$\psi(\| x_{hk} - x_p \|) = \sqrt{1 + (c \| x_{hk} - x_p \|)^2}$$

in case of GA, IQ, and MQ RBF, respectively.

Matrix form of eq. (8) is:

$$\underbrace{\begin{bmatrix} \psi_{h1}^{(m)}(x_h) \\ \psi_{h2}^{(m)}(x_h) \\ \vdots \\ \psi_{hn_h}^{(m)}(x_h) \end{bmatrix}}_{\boldsymbol{\psi}_{n_h}^{(m)}} = \underbrace{\begin{bmatrix} \psi_{h1}(x_{h1}) & \psi_{h2}(x_{h1}) & \cdots & \psi_{hn_h}(x_{h1}) \\ \psi_{h1}(x_{h2}) & \psi_{h2}(x_{h2}) & \cdots & \psi_{hn_h}(x_{h2}) \\ \vdots & \vdots & \ddots & \vdots \\ \psi_{h1}(xh_{n_h}) & \psi_{h2}(x_{hn_h}) & \cdots & \psi_{hn_h}(xh_{n_h}) \end{bmatrix}}_{\mathbf{A}_{n_h}} \underbrace{\begin{bmatrix} \lambda_{h1}^{(m)} \\ \lambda_{h2}^{(m)} \\ \vdots \\ \lambda_{hn_h}^{(m)} \end{bmatrix}}_{\boldsymbol{\lambda}_{n_h}^{(m)}} \tag{9}$$

where $\psi_p(x_k) = \psi(\| x_k - x_p \|), p = h1, h2, \ldots, hn_h$, for each $k = i1, h2, \ldots, hn_h$. Equation (9) can be written:

$$\boldsymbol{\psi}_{n_h}^{(m)} = \mathbf{A}_{n_h} \boldsymbol{\lambda}_{n_h}^{(m)} \tag{10}$$

From eq. (10), we obtain:

$$\boldsymbol{\lambda}_{n_h}^{(m)} = \mathbf{A}_{n_h}^{-1} \boldsymbol{\psi}_{n_h}^{(m)} \tag{11}$$

Equations (7) and (11) imply:

$$W^{(m)}(x_h) = [\boldsymbol{\lambda}_{n_h}^{(m)}]^T \mathbf{W}_{n_h}$$

where

$$\mathbf{W}_{n_h} = [W(x_{h1}), W(x_{h2}), \ldots, W(x_{hn_h})]^T$$

In case of 2-D, the derivatives of $W(x, y, t)$ regarding x and y are approximated in the comparative manner:

$$W_x^{(m)}(x_h, y_h) \approx \sum_{k=1}^{n_h} [\gamma_k^{(m)} W(x_{hk}, y_{hk}], \quad h = 1, 2, \ldots, N^2 \tag{12}$$

$$W_y^{(m)}(x_h, y_h) \approx \sum_{k=1}^{n_h} [\eta_k^{(m)} W(x_{hk}, y_{hk})], \quad h = 1, 2, \ldots, N^2 \tag{13}$$

To find out the relating coefficients $\gamma_k^{(m)}$ and $\eta_k^{(m)}$ ($k = 1, 2,\ldots, n_h$), we continue:

$$\boldsymbol{\gamma}_{n_h}^{(m)} = \mathbf{A}_{n_h}^{-1}\boldsymbol{\Phi}_{n_h}^{(m)} \tag{14}$$

$$\boldsymbol{\eta}_{n_h}^{(m)} = \mathbf{A}_{n_h}^{-1}\boldsymbol{\Phi}_{n_h}^{(m)} \tag{15}$$

The previous technique can be rehashed for 3-D case, *etc.*

In 3-D geometries the local central stencils are developed around each center $\bar{z}_h$ whose schematic is appeared in fig. 1.

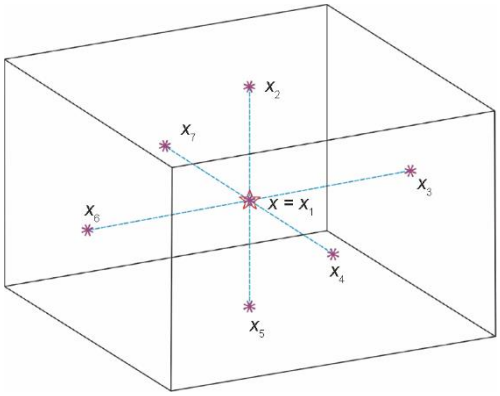

Figure 1. Schematics view in 3-D for $n_i = 7$ of local stencils [34]

Discretization of time derivatives

The time derivative $[\partial^\alpha W(\bar{z},t)]/\partial t^\alpha$ is discretized by using Liouville-Caputo derivative [48]. The Liouville-Caputo fractional derivative for $\alpha \in (0,1)$ is:

$$\frac{\partial^\alpha W(\bar{z},t)}{\partial t^\alpha} = \begin{cases} \dfrac{1}{\Gamma(1-\alpha)}\displaystyle\int_0^t \frac{\partial W(\bar{z},\vartheta)}{\partial \vartheta}(t-\vartheta)^{-\alpha}\,\mathrm{d}\vartheta, & 0<\alpha<1 \\ \dfrac{\partial W(\bar{z},t)}{\partial t} & \alpha = 1 \end{cases}$$

For the interval $[0, t]$, $Q + 1$ is considered as equally spaced time intervals $t_0, t_1,\ldots, t_Q$, such that $t_q = q\tau$, $n = 0, 1, 2,\ldots, Q$, τ is the time step and to approximate the first-order derivative involved in the time fractional term, finite difference scheme is used:

$$\begin{aligned} \frac{\partial^\alpha W(\bar{z},t_{q+1})}{\partial t^\alpha} &= \frac{1}{\Gamma(1-\alpha)}\int_0^{t_{q+1}} \frac{\partial W(\bar{z},\vartheta)}{\partial \vartheta}(t_{q+1}-\vartheta)^{-\alpha}\,\mathrm{d}\vartheta \\ &= \frac{1}{\Gamma(1-\alpha)}\sum_{s=0}^{q}\int_{s\tau}^{(s+1)\tau} \frac{\partial W(\bar{z},\vartheta)}{\partial \vartheta}(t_{s+1}-\vartheta)^{-\alpha}\,\mathrm{d}\vartheta \\ &\approx \frac{1}{\Gamma(1-\alpha)}\sum_{s=0}^{q}\int_{s\tau}^{(s+1)\tau} \frac{\partial W(\bar{z},\vartheta_s)}{\partial \vartheta}(t_{s+1}-\vartheta)^{-\alpha}\,\mathrm{d}\vartheta \end{aligned}$$

The term $[\partial W(\bar{z},\vartheta_s)]/\partial\vartheta$ is approximated:

$$\frac{\partial W(\bar{z},\vartheta_s)}{\partial \vartheta} = \frac{W(\bar{z},\vartheta_{s+1}) - W(\bar{z},\vartheta_s)}{\vartheta} + \mathcal{O}(\tau)$$

Then

$$\frac{\partial^{\alpha} W(\bar{z},t_{q+1})}{\partial t^{\alpha}} \approx \frac{1}{\Gamma(1-\alpha)}\sum_{s=0}^{q}\frac{W(\bar{z},t_{s+1})-W(\bar{z},t_{s})}{\tau}\int_{s\tau}^{(s+1)\tau}(t_{s+1}-\vartheta)^{-\alpha}\,\mathrm{d}\vartheta$$

$$= \frac{1}{\Gamma(1-\alpha)}\sum_{s=0}^{q}\frac{W(\bar{z},t_{q+1-s})-W(\bar{z},t_{q-s})}{\tau}\int_{s\tau}^{(s+1)\tau}(t_{s+1}-\vartheta)^{-\alpha}\,\mathrm{d}\vartheta$$

$$= \begin{cases} \dfrac{\tau^{-\alpha}}{\Gamma(2-\alpha)}(W^{q+1}-W^{q}) + \dfrac{\tau^{-\alpha}}{\Gamma(2-\alpha)}\displaystyle\sum_{s=1}^{q}(W^{q+1-s}-W^{q-s})[(s+1)^{1-\alpha}-s^{1-\alpha}], & q\geq 1 \\ \dfrac{\tau^{-\alpha}}{\Gamma(2-\alpha)}(W^{1}-W^{0}), & q=0 \end{cases}$$

Letting $a_0 = \tau^{-\alpha}/[\Gamma(2-\alpha)]$ and $b_s = (s+1)^{1-\alpha} - s^{1-\alpha}$, $s = 0, 1, \ldots, q$, we can write the above equation in more precise form:

$$\frac{\partial^{\alpha} W(\bar{z},t_{q+1})}{\partial t^{\alpha}} \approx \begin{cases} a_0(W^{q+1}-W^{q}) + a_0\displaystyle\sum_{s=1}^{q} b_s(W^{q+1-s}-W^{q-s}), & q\geq 1 \\ a_0(W^{1}-W^{0}), & q=0 \end{cases}$$

Numerical results

In this section, the numerical results of the 3-D time fraction convection-diffusion model equations using the proposed LMM. The GA, IQ, and MQ RBF are used for space discretization in all numerical simulation. All numerical experiments are performed using local supported domain $n_i = 7$. All the computations are performed on HP (ProBook) PC Laptop with an Intel(R) Core(TM) i5-4210M CPU 2.60 GHz 2.60 GHz 4 GB RAM. The accuracy is measure through $|\varepsilon|$, max(ε), and ε norms which are define:

$$\begin{aligned} |\varepsilon| &= \left|\hat{\mathbb{W}} - W\right|, \\ \max(\varepsilon) &= \max\left(|\varepsilon|\right), \\ \varepsilon &= \sqrt{\frac{\sum_{i=1}^{N}(\hat{\mathbb{W}}_i - W_i)^2}{\sum_{i=1}^{N}(\hat{\mathbb{W}}_i)^2}} \end{aligned} \tag{16}$$

where $\hat{\mathbb{W}}$ is exact solution and W is the approximate solution.

Test problem 1. Consider eq. (1) as 3-D unsteady convection-diffusion having exact solution for $\alpha = 1$:

$$W(\bar{z},t) = e^{[Dt-E(x+y+z)]}, \quad t\geq 0, \quad (x,y,z)\in[-1,1]^3 \tag{17}$$

where $E = \sqrt{(D/6)}, D = 1/10, F(\bar{z},t) = 0,$ and $\gamma = (-E,-E,-E)$.

The numerical results for *Test problem 1* are obtained by the LMM in explicit form and are shown in tab. 1. Three different RBF (GA, IQ, and MQ) with shape parameter value

$c = 100$, are used. The error is measure in terms of $\max(\varepsilon)$ and ε for this test problem by taking different nodes N, time step size $\tau = 0.002$ and final time $t = 1$. This shows that the suggested method gives good accuracy and also we can observed that the accuracy of mentioned RBF are all most the same. A comparison of exact and numerical results are shown in fig. 2(a), while in fig. 2(b) for different values of α the results are shown for $x = y = z$.

Table 1. Numerical results of convection-diffusion equation for *Test problem 1*

	$N = 125$		$N = 512$		$N = 1331$	
RBF	$\max(\varepsilon)$	ε	$\max(\varepsilon)$	ε	$\max(\varepsilon)$	ε
GA	$1.0325\cdot10^{-5}$	$1.3020\cdot10^{-6}$	$2.0926\cdot10^{-6}$	$4.1421\cdot10^{-7}$	$8.0243\cdot10^{-8}$	$8.1723\cdot10^{-9}$
IQ	$1.1047\cdot10^{-5}$	$1.3935\cdot10^{-6}$	$2.2963\cdot10^{-6}$	$4.5542\cdot10^{-7}$	$4.5976\cdot10^{-8}$	$8.9339\cdot10^{-9}$
MQ	$1.0109\cdot10^{-5}$	$1.2746\cdot10^{-6}$	$1.9962\cdot10^{-6}$	$3.9469\cdot10^{-7}$	$2.7539\cdot10^{-7}$	$7.6212\cdot10^{-8}$

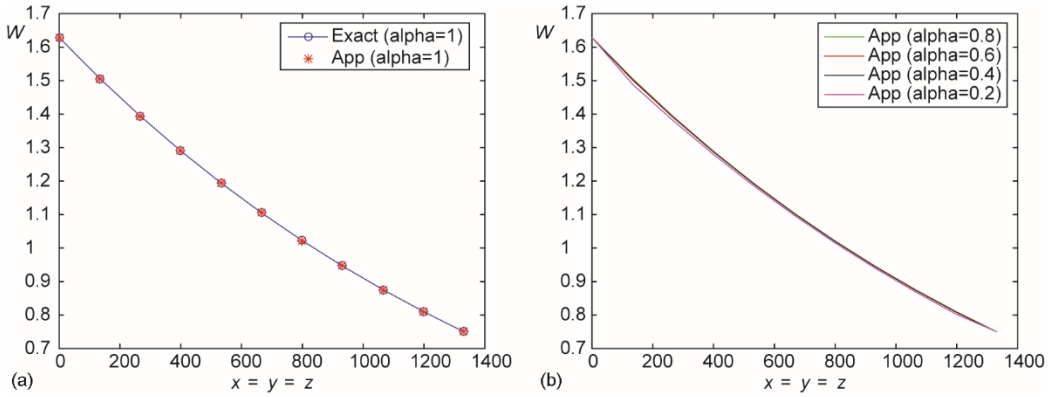

Figure 2. Numerical solution of the LMM using GA RBF at $t = 1$ for *Test problem 1*

Test problem 2. Consider eq. (1) with $\gamma = 0$, having exact solution for $\alpha = 0.9$ is given:

$$W(\bar{z},t) = t^2 \mathrm{e}^{(x+y+z)}, \quad t \geq 0, \quad (x,y,z) \in [0,1]^3 \tag{18}$$

and the source term is:

$$F(\bar{z},t) = \frac{\Gamma(3)}{\Gamma(2.1)} t^{1.1} \mathrm{e}^{(x+y+z)} - 3t^2 \mathrm{e}^{(x+y+z)}$$

The numerical results for the *Test problem 2* using GA RBF in terms of $\max(\varepsilon)$ and ε norms, are described in tab. 2 for shape parameter value $c = 10$ and $t = 1$. It can be seen in this test problem as well that the LMM gives accurate results.

Table 2. Simulation results of the LMM for *Test problem 2*

	$N = 125$		$N = 216$		$N = 512$	
RBF	$\max(\varepsilon)$	ε	$\max(\varepsilon)$	$\max(\varepsilon)$	ε	$\max(\varepsilon)$
GA	$8.5305\cdot10^{-4}$	$9.3340\cdot10^{-5}$	$6.0538\cdot10^{-4}$	$7.5199\cdot10^{-5}$	$2.8195\cdot10^{-4}$	$4.5463\cdot10^{-5}$

A comparison of exact and numerical results using GA RBF for $N = 125$ at $t = 0.5$, and taking the values of $z = 0$, 0.25, 0.5, 0.75, and 1 are shown in fig. 3. This figure is also the evidence of the proposed method for better accuracy. The error, $|\varepsilon|$, are also shown in fig. 4 using $N = 729$ and $T = 0.5$. The LMM is testified on irregular domain with non-uniform nodes as shown in fig. 5. The numerical results are shown in tab. 3 for different final time. It is clear from the table that the LMM gives good numerical results irrespective of the domain and nodel points.

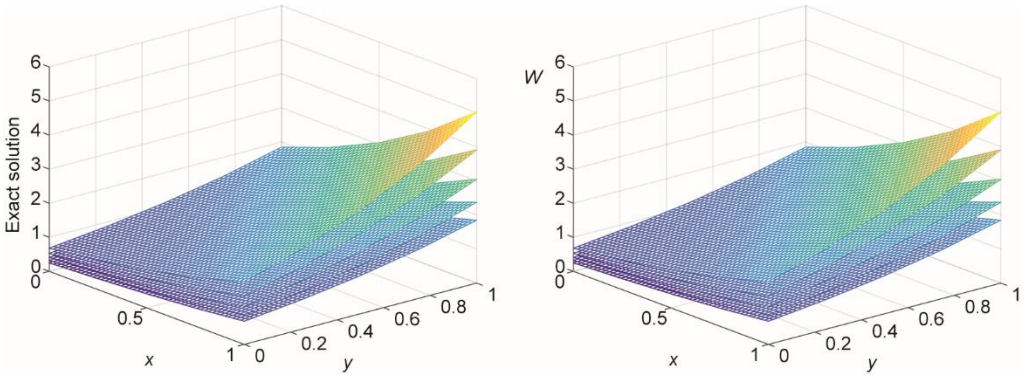

Figure 3. Numerical solution of the LMM using GA RBF taking $N = 125$ and $z = 0$, 0.25, 0.5, 0.75, and 1 for *Test problem 2*

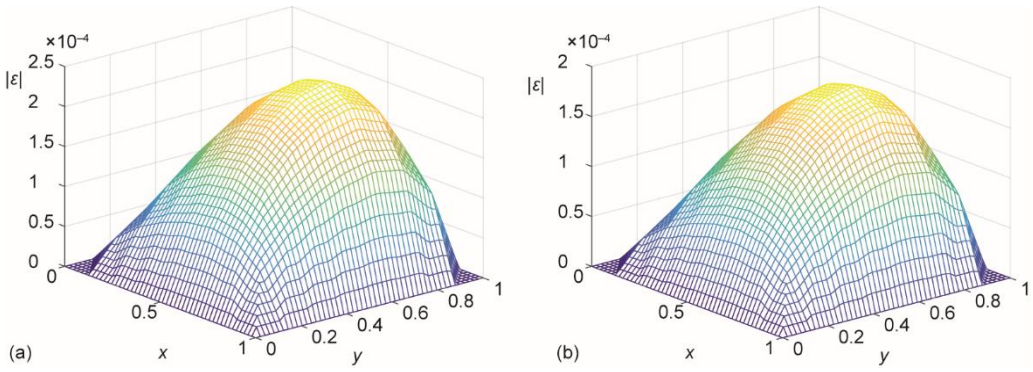

Figure 4. Error in term of $|\varepsilon|$ of the LMM using IQ (a) and MQ (b) at $z = 0.5$ for *Test problem 2*

Test problem 3. Consider the 3-D Burgers' eq. (4). For $\alpha = 1$ the exact solutions is:

$$W(\bar{z},t) = 1 - \frac{1}{2}\left[1 + \exp\left(\frac{\frac{-3t}{4} - x + y + z}{4\beta}\right)\right]^{-1}, \quad t \geq 0, \quad (x,y,z) \in [0,1]^3 \tag{19}$$

Figure 6 shows $|\varepsilon|$ error norm of the LMM by taking $N = 1331$ and $\beta = 1$ for *Test problem 3*. The figure shows that the proposed LMM gives good results in this test problem as well for all the three RBF. The numerical results for computational domain given in fig. 5 in terms of max(ε) and ε error norms for *Test problem 3* are given in tab. 4 with $\beta = 1$ and

N = 2046. Figure 7 shows the exact *vs.* numerical solution of the LMM which is self explanatory. The numerical results for N = 9261, β = 0.02, α = 0.8, and α = 0.9 are shown in fig. 8 at different values of z = 0, 0.2, 0.4, 0.6, 0.8, and 1.

Table 3. Numerical results on computational domain in fig. 5 for *Test problem 2*

	T = 0.1		T = 0.5		T = 1	
RBF	max(ε)	ε	max(ε)	ε	max(ε)	ε
GA	$1.1749\cdot10^{-4}$	$2.6781\cdot10^{-4}$	$3.3914\cdot10^{-3}$	$4.5966\cdot10^{-4}$	$1.4041\cdot10^{-2}$	$5.3864\cdot10^{-4}$

Table 4. Simulation results on computational domain in fig. 5 for *Test problem 3*

	T = 0.1		T = 0.5		T = 1	
RBF	max(ε)	ε	max(ε)	ε	max(ε)	ε
MQ	$6.8692\cdot10^{-5}$	$1.4177\cdot10^{-5}$	$1.5408\cdot10^{-4}$	$7.5077\cdot10^{-5}$	$3.4544\cdot10^{-4}$	$1.6527\cdot10^{-4}$

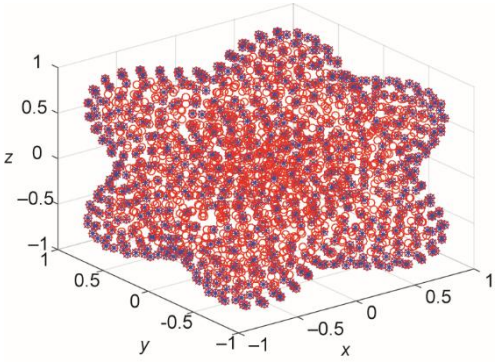

Figure 5. Computational domain with non-uniform nodes [34]

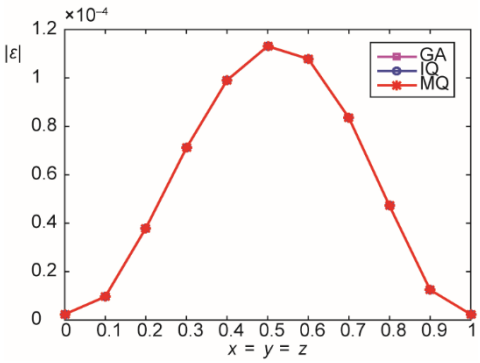

Figure 6. Error in term of $|\varepsilon|$ at $x = y = z$ for *Test problem 3*

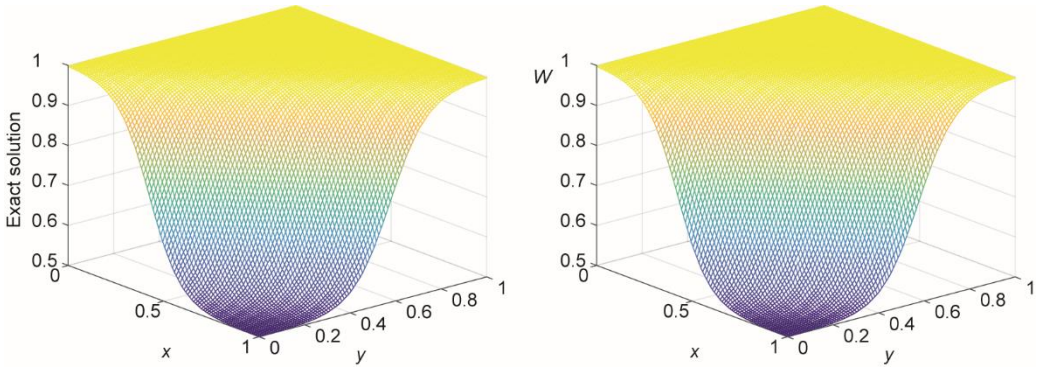

Figure 7. Exact *vs.* numerical solutions with β = 0.02 at z = 0.5 for *Test problem 3*

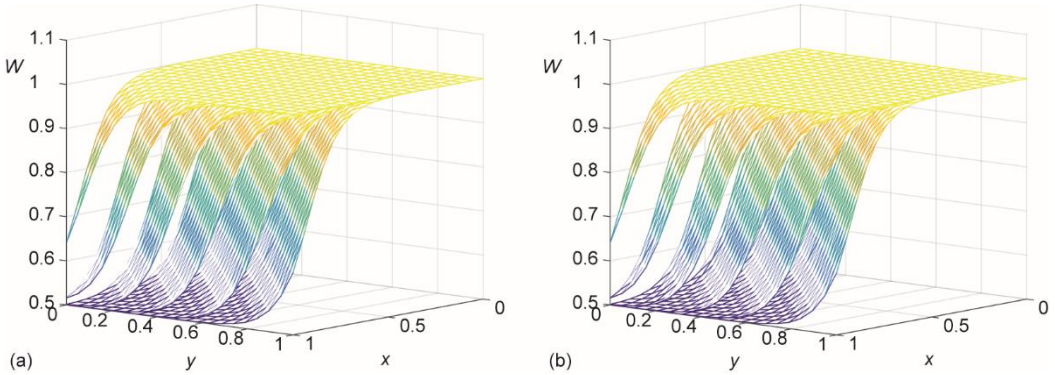

Figure 8. Numerical solution for α = 0.8 (a) and α = 0.9 (b) at z = 0, 0.2, 0.4, 0.6, 0.8, and 1 for *Test problem 3*

Conclusion

In this work, we have applied a local meshless method based on RBF as a modern powerful numerical method to investigate 3-D time dependent fractional convection-diffusion PDE models. The time derivative part is defined and simplified in Liouville-Caputo sense and the scheme is constructed for $0 < \alpha < 1$. Various test problems have been considered on regular and irregular domains to check the accuracy of the proposed scheme. The numerical results are the evidence that the suggested LMM is a flexible interpolation method as it produce the coefficient matrix well-conditioned. In light of the current work we can say that the proposed technique is powerful and effective to find the numerical solutions of 3-D time dependent fractional PDE, so it can be also applied to a wide range of complex problems that occur in natural sciences and engineering.

References

[1] Samko, S. G., *et al.*, *Fractional Integrals and Derivatives* (in Russian), Gordon and Breach, Yverdon, Switzerland, 1993
[2] Kilbas, A. A., *et al.*, *Theory and Applications of Fractional Differential Equations*, Vol. 204 (North-Holland Mathematics Studies), Elsevier (North-Holland) Science Publishers, Amsterdam, London and New York, 2006
[3] Srivastava, H. M., Fractional-Order Derivatives and Integrals: Introductory Overview and Recent Developments, *Kyungpook Mathematical Journal, 60* (2020), 1, pp. 73-116
[4] Srivastava, H. M., *et al.*, Dynamic Response Analysis of Fractionally-Damped Generalized Bagley-Torvik Equation Subject to External Loads, *Russian Journal of Mathematical Physics, 27* (2020), May, pp. 254-268
[5] Ahmad, H., Khan, T. A., Variational Iteration Algorithm-i with an Auxiliary Parameter for Wave-Like Vibration Equations, *Journal of Low Frequency Noise, Vibration and Active Control, 38* (2019), 3-4, pp. 1113-1124
[6] Mahto, L., *et al.*, Approximate Controllability of Sub-Diffusion Equation with Impulsive Condition, *Mathematics, 7* (2019), 2, 190
[7] Yang, X.-J., *et al.*, A New Fractional Derivative without Singular Kernel: Application to the Modelling of the Steady Heat Flow, *Thermal Science, 20* (2016), 2, pp. 753-756
[8] Ahmad, H., *et al.*, Analytic Approximate Solutions for Some Nonlinear Parabolic Dynamical Wave Equations, *Journal of Taibah University for Science, 14* (2020), 1, pp. 346-358
[9] El-Dib, Y., Stability Analysis of a Strongly Displacement Time-Delayed Duffing Oscillator Using Multiple Scales Homotopy Perturbation Method, *Journal of Applied and Computational Mechanics, 4* (2018), 4, pp. 260-274

[10] Jena, R. M., *et al.*, Dynamic Response Analysis of Fractionally Damped Beams Subjected to External Loads Using Homotopy Analysis Method, *Journal of Applied and Computational Mechanics, 5* (2019), 2, pp. 355-366
[11] Yokus, A., *et al.*, Hyperbolic Type Solutions for the Couple Boiti-Leon-Pempinelli System, *Facta Universitatis, Series: Mathematics and Informatics, 35* (2020), 2, pp. 523-531
[12] Yokus, A., *et al.*, Construction of Different Types Analytic Solutions for the Zhiber-Shabat Equation, *Mathematics, 8* (2020), 6, 908
[13] Srivastava, H. M., Saad, K. M., Some New Models of the Time-Fractional Gas Dynamics Equation, *Advanced Mathematical Models and Applications, 3* (2018), 1, pp. 5-17
[14] Bisheh-Niasar, M., Ameri, M. A., Moving Mesh Non-Standard Finite Difference Method for Non-Linear Heat Transfer in a Thin Finite Rod, *Journal of Applied and Computational Mechanics, 4* (2018), 3, pp. 161-166
[15] Zhukovsky, K. V., Srivastava, H. M., Analytical Solutions for Heat Diffusion beyond Fourier Law, *Applied Mathematics and Computation, 293* (2017), Jan., pp. 423-437
[16] Jassim, H. K., Baleanu, D., A Novel Approach for Korteweg-de Vries Equation of Fractional Order, *Journal of Applied and Computational Mechanics, 5* (2019), 2, pp. 192-198
[17] Ahmad, H., Variational Iteration Method with an Auxiliary Parameter for Solving Differential Equations of the Fifth Order, *Nonlinear Science Letters A, 9* (2018), 1, pp. 27-35
[18] Inc, M., *et al.*, Modified Variational Iteration Method for Straight Fins with Temperature Dependent Thermal Conductivity, *Thermal Science, 22* (2018), Suppl 1, pp. S229-S236
[19] Kilicman, A., *et al.*, Analytic Approximate Solutions for Fluid Flow in the Presence of Heat and Mass Transfer, *Thermal Science, 22* (2018), Suppl. 1, pp. S259-S264
[20] Srivastava, H. M., *et al.*, Stability of Traveling Waves Based upon the Evans Function and Legendre Polynomials, *Applied Sciences, 10* (2020), 3, 846
[21] Yang, X.-J., *et al.*, General Fractional-Order Anomalous Diffusion with Non-Singular Power-Law Kernel, *Thermal Science, 21* (2017), 1, pp. 1-9
[22] Kucukarslan-Yuzbasi, Z., *et al.*, On Exact Solutions for New Coupled Nonlinear Models Getting Evolution of Curves in Galilean Space, *Thermal Science, 23* (2019), Suppl. 1, pp. S227-S233
[23] Saravanan, A., Magesh, N., A Comparison between the Reduced Differential Transform Method and the Adomian Decomposition Method for the Newell-Whitehead-Segel Equation, *Journal of the Egyptian Mathematical Society, 21* (2013), 3, pp. 259-265
[24] Akgul, A., *et al.*, New Method for Investigating the Density-Dependent Diffusion Nagumo Equation, *Thermal Science, 22* (2018), Suppl. 1, pp. S143-S152
[25] Yang, X.-J., *et al.*, A New Numerical Technique for Solving the Local Fractional Diffusion Equation: Two-Dimensional Extended Differential Transform Approach, *Applied Mathematics and Computation 274* (2016), Feb., pp. 143-151
[26] Yang, X.-J., *et al.*, Exact Travelling Wave Solutions for the Local Fractional Two-Dimensional Burgers-Type Equations, *Computers & Mathematics with Applications, 73* (2017), 2, pp. 203-210
[27] Ahmad, I., *et al.*, Numerical Simulation of Partial Differential Equations via Local Meshless Method, *Symmetry, 11* (2019), 2, 257
[28] Khan, M. N., *et al.*, A Local Meshless Method for the Numerical Solution of Space-Dependent Inverse Heat Problems, *Mathematical Methods in the Applied Sciences*, On-line first, https://doi.org/10.1002/mma.6439, 2020
[29] Oguntala, G., Abd-Alhameed, R., Thermal Analysis of Convective-Radiative Fin with Temperature-Dependent Thermal Conductivity Using Chebychev Spectral Collocation Method, *Journal of Applied and Computational Mechanics, 4* (2018), 2, pp. 87-94
[30] Wendland, H., *Approximation Scattered Data*, Cambridge University Press, Cambridge, London and New York, 2005
[31] Shen, Q., Local RBF-Based Differential Quadrature Collocation Method for the Boundary Layer Problems, *Engineering Analysis with Boundary Elements 34* (2010), 3, pp. 213-228
[32] Yan, X., Pan, Y., Performance Analysis of Heat Accumulation of Solar Thermal Generator Units by Computer Numerical Simulation, *Thermal Science, 24* (2020), 5B, pp. 3279-3287
[33] Shu, C., *Differential Quadrature and Its Application in Engineering*, Springer-Verlag, Berlin, Heidelberg and New York, 2000
[34] Ahmad, I., *et al.*, Local RBF Method for Multi-Dimensional Partial Differential Equations, *Computers & Mathematics with Applications, 74* (2017), 2, pp. 292-324

[35] Siraj-ul-Islam, Ahmad, I., A Comparative Analysis of Local Meshless Formulation for Multi-Asset Option Models, *Engineering Analysis with Boundary Elements, 65* (2016), Apr., pp. 159-176
[36] Khan, M. N., *et al.*, A Radial Basis Function Collocation Method for Space-Dependent Inverse Heat Problems, *Journal of Applied and Computational Mechanics*, On-line first, https://doi.org/10.22055/JACM. 2020. 32999.2123, 2020
[37] Mohebbi, A., *et al.*, The Use of a Meshless Technique Based on Collocation and Radial Basis Functions for Solving the Time Fractional Nonlinear Schrodinger Equation Arising in Quantum Mechanics, *Engineering Analysis with Boundary Elements, 37* (2013), 2, pp. 475-485
[38] Piret, C. C., Hanert, E., A Radial Basis Functions Method for Fractional Diffusion Equations, *Journal of Computational Physics, 238* (2013), Apr., pp. 71-81
[39] Mohebbi, A., *et al.*, Solution of Two-Dimensional Modified Anomalous Fractional Sub-Diffusion Equation via Radial Basis Functions (RBF) Meshless Method, *Engineering Analysis with Boundary Elements, 38* (2014), Jan., pp. 72-82
[40] Hosseini, V. R., *et al.*, Numerical Solution of Fractional Telegraph Equation by Using Radial Basis Functions, *Engineering Analysis with Boundary Elements, 38* (2014), Jan., pp. 31-39
[41] Wei, S., *et al.*, Implicit Local Radial Basis Function Method for Solving Two-Dimensional Time Fractional Diffusion Equations, *Thermal Science, 19* (2015), Suppll. 1, pp. S59-S67
[42] Ghehsareh, H. R., *et al.*, A Meshfree Method Based on the Radial Basis Functions for Solution of Two-Dimensional Fractional Evolution Equation, *Engineering Analysis with Boundary Elements, 61* (2015), Dec., pp. 52-60
[43] Aslefallah, M., Shivanian, E., Nonlinear Fractional Integro-Differential Reaction-Diffusion Equation via Radial Basis Functions, *The European Physical Journal Plus, 130* (2015), 3, 47
[44] Kumar, A., *et al.*, A Meshless Local Collocation Method for Time Fractional Diffusion Wave Equation, *Computers & Mathematics with Applications, 78* (2019), 6, pp. 1851-1861
[45] Wei, S., *et al.*, A Local Radial Basis Function Collocation Method to Solve the Variable-Order Time Fractional Diffusion Equation in a Two-Dimensional Irregular Domain, *Numerical Methods for Partial Differential Equations, 34* (2018), 4, pp. 1209-1223
[46] Dehghan, M., *et al.*, An Implicit RBF Meshless Approach for Solving the Time Fractional Nonlinear Sine-Gordon and Klein-Gordon Equations, *Engineering Analysis with Boundary Elements, 50* (2015), Jan., pp. 412-434
[47] Avazzadeh, Z., *et al.*, Radial Basis Functions and FDM for Solving Fractional Diffusion-Wave Equation, *Iranian Journal of Science and Technology Transactions A: Science, 38* (2014), 3, pp. 205-212
[48] Caputo, M., Linear Models of Dissipation Whose Q is Almost Frequency Independent. II, *Geophysical Journal International, 13* (1967), 5, pp. 529-539

Paper submitted: February 2, 2020
Paper revised: May 2, 2020
Paper accepted: July 2, 2020

© 2021 Society of Thermal Engineers of Serbia.
Published by the Vinča Institute of Nuclear Sciences, Belgrade, Serbia
This is an open access article distributed under the CC BY-NC-ND 4.0 terms and conditions.